Phase transformations during the zeolitization of fly ashes

J.D. Monzón[a,c], A.M. Pereyra[a], M.S. Conconi[b], E.I. Basaldella[a,*]

[a] Centro de Investigación y Desarrollo en Ciencias Aplicadas—Dr. Jorge J. Ronco, CINDECA (CONICET-CIC-UNLP), Calle 47 N° 257, La Plata, Argentina
[b] Centro de Tecnología de Recursos Minerales y Cerámicos, Cno. Centenario y 506, CC 49, 1897 M. B. Gonnet, Argentina
[c] Centro de Investigación y Desarrollo en Ciencia y Tecnología de Materiales (CITEMA), Facultad Regional La Plata, UTN, La Plata, Argentina

ABSTRACT

The reactivity of a fly ash discarded from a thermoelectric power station was evaluated in terms of its hydrothermal conversion into NaA-containing products. The influence of ash pretreatments and the effect of changes in the synthesis mixture composition on the evolution of the solid phase toward its conversion into zeolitic materials were studied. Activation by milling was not as effective as alkaline fusion. The highest levels of fly ash reactivity were obtained by applying an alkaline fusion treatment using sodium carbonate at 800°C. It was observed that this particular ash activatiorn induces a solid reordering that generates crystalline materials identified as $NaAlSiO_2$ polymorphs that in turn are easily transformed into zeolite structures. Synthesis conditions for ash zeolitization as high as 60% were established.

1. Introduction

The increased demand for electricity has created the need to build large thermoelectric power plants where coal is the primary fuel used. Forecasts of the World Coal Association indicate that, in the coming years, approximately 44% of worldwide exploitation of coal will be used for electric power generation. In the near future, this fact suggests an increase in coal consumption and consequently, the generation of a significant amount of solid combustion residue (fly ash and bottom ash). It is estimated that the combustion of 1 tn. of coal generates an average of 80–250 kg of solid waste depending on the coal type used. Fly ash represents almost 70% of all coal combustion products [1].

Currently, fly ash is collected in the hoppers of electrostatic precipitators and subsequently transported to the storage sites. Of all the ash produced, less than 20% is recycled, mainly used in the cement industry; the rest is disposed of in landfills or lagoons, generating negative environmental impacts.

At present, different investigations are focused on developing new recycling techniques for coal fly ash. In this way, the presence of inorganic compounds such as silicates or vitreous aluminosilicates and some crystalline phases (i.e., mullite, quartz) in industrial fly ash makes them suitable for use as raw material in the synthesis of different types of zeolites [2–7].

For ash conversion processes, several authors propose different ways to obtain specific zeolitic products. For NaA-type zeolite (NaA), the procedures range from the application of a direct conversion by hydrothermal synthesis [8] to microwave assisted hydrothermal conversion [9] and ultrasound assisted hydrothermal conversion [10,11]. Ash treatments applied before synthesis are also common. The fusion followed by hydrothermal treatment [12], with or without microwave or ultrasound assistance (indirect conversion), has also been studied [13,14].

This paper describes the use of two different procedures for improving ash reactivity: milling and alkaline fusion using sodium carbonate. The influence of two activation methodologies that can be easily applied to the industrial residue on the hydrothermal zeolitization of fly ashes was analyzed, along with different synthesis mixture compositions. A fly ash from a thermoelectric power station, usually discarded as a non-valuable residue, with or without pretreatments (milling or calcination with Na_2CO_3), was alkaline-treated using different chemical composition media, aged and reacted under controlled conditions of temperature at autogenous pressure. Since the hydrothermal treatment in NaOH aqueous media leads to the crystallization of NaP zeolite ($Na_6[(AlO_2)_6(SiO_2)_{10}].15H_2O$) [15] and considering that the technological applications of zeolite NaP are fewer than those of zeolite

* Corresponding author.
  E-mail addresses: eib@quimica.unlp.edu.ar, ebasaldella@hotmail.com
(E.I. Basaldella).

A ($Na_{12}[(AlO_2)_{12}(SiO_2)_{12}]$ $27H_2O$), the composition of the synthesis mixture was optimized for obtaining type A zeolite instead of NaP. Zeolite growth during the hydrothermal synthesis was followed by X-ray diffraction (XRD), scanning electron microscopy (SEM) and energy-dispersive X-ray analysis (EDX).

2. Experimental

2.1. Materials

Fly ash. A fly ash discarded from the thermoelectric power station of San Nicolás, Buenos Aires, Argentina, was used. For this study, particles possessing a size fraction between 60 μm and 100 μm were selected by screening."

2.2. Physicochemical characterization

The structural characterization of crystalline materials (starting fly ash, the products obtained after pretreatments, and those resulting from hydrothermal synthesis) was carried out by XRD. The diffraction patterns were obtained in Bruker D2 Phaser equipment (30 kV, 10 mA, Cu Kα by Ni filter, step width 0.04°, and counting time 2.5 s/step). The types of zeolite and other crystalline phases obtained were determined by comparing diffraction profiles with published data [16]. The Rietveld method [17] and the program "FULLPROF" [18] were used for the quantitative determination of the crystalline components. The morphology and semiquantitative chemical composition of the solid samples were obtained by SEM using a Philips 505 microscope equipped with an EDX spectrometer".

2.3. Activation pretreatments and hydrothermal synthesis. Zeolite conversion process

Fly ash was subjected to different pretreatments, including high-energy ball milling or calcination with or without Na_2CO_3.

For milling pretreatment, a Herzog HSM 100 oscillating mill was used. The influence of impact time on the reactivity of the samples was evaluated. Samples at treatment times of 60, 300, 600 and 3600 s were obtained.

For the alkaline fusion pretreatment, samples containing ash and sodium carbonate mixed in different proportions (0, 25, 50 or

75 wt% of Na_2CO_3, Carlo Erba p.a.) were heat-treated according to the method described in [19]. Na_2CO_3 was selected as the fusion salt based on economical considerations, because of its cost-effective replacement by a cheaper natural sodium carbonate source (i.e., trona). Briefly, the ash/carbonate mixtures were prepared under sonication. After 5 min of mixing, the solids were calcined under static conditions at 800 ± 10 °C, for 2 h. To evaluate the influence of the time used for the heat treatment, an additional sample containing ash/Na_2CO_3 = 1/1 (wt) was heated for 12 h. Subsequently, each of the pretreated samples (9.6 g) was placed in contact with the activation mixture in a 250 ml polypropylene reactor. The original fly ash was also checked. The activation mixture was formed by appropriate amounts of NaOH (Carlo Erba p.a.) and deionized water; $NaAlO_2$ commercial solution (36.5% Al_2O_3, 29.6% Na_2O, 33.9% H_2O) was optionally added as extra aluminum source at the beginning of the synthesis in order to obtain NaA zeolite as the main product. Al_2O_3 quantities are detailed in Table 1. Each sample was mixed with a magnetic stirrer for 30 min and aged at room temperature for 48 h. Then, the mixture was placed in a conventional air oven at 100 °C. The course of the reaction was followed by taking aliquots at different times, 0, 3, 5, 23, 31, and 48 h. The solid products obtained were washed and dried in a conventional air oven at 110 °C.

3. Results and discussion

3.1. Fly ash pretreatments

Compounds. According to the XRD analysis, the fly ash contained mullite ($Al_{4.52}Si_{1.48}O_{9.74}$) 17.2 wt%, quartz ($SiO_2$) 5.5 wt%, hematite ($Fe_2O_3$) 1.5 wt%, calcite ($CaCO_3$) 1.6 wt%, and an amorphous phase, 74.2 wt%. The chemical analysis of the original fly ash revealed the following composition (wt%): SiO_2 = 62.8, Al_2O_3 = 27.4, Na_2O = 0.8, Fe_2O_3 = 3.5, TiO_2 = 1.4, MgO = 1.6, K_2O = 0.7, and CaO = 1.8.

In Fig. 1, the X-ray diffraction patterns corresponding to the original fly ash (a) and to the fly ash after 3600 s of milling (b) are depicted. The diffraction patterns for the ash heated for 2 h at 800 °C or subjected to shorter milling times (60, 300 and 600 s) (not shown) indicated no change with respect to (a), i.e., heating or milling did not alter the ash crystalline structure. Nevertheless, some changes were noted when the milling time was increased. The diffraction pattern obtained after 3600 s of milling (b) clearly

Table 1
Pretreatments, synthesis mixture compositions and maximum conversion in zeolite A.

Sample	Pretreatment			Activation solution, g			NaA maximum conversion, %		Type
	Milling time, sec	Calcination time at 800 °C, h	Na_2CO_3 (wt%)[a]	H_2O	[b]Al_2O_3	Na_2O	Reaction time, h	%	
D7	0	2	50	88.8	0.43	3.1	23	64	A+Tr HS
D8	0	2	50	88.8	0.43	1.55	48	57	A+HS
D9	0	2	50	88.8	0.32	3.1	31	20	A+HS+Tr X
D10	0	2	50	88.8	0.54	3.1	5	64	A+Tr HS
D11	0	2	50	88.8	0.43	4.65	3	57	A+Tr HS
D12	0	2	50	133.2	0.43	3.1	23	56	A+Tr HS
D13	0	2	50	44.4	0.43	3.1	3	56	A+Tr HS
D14	0	2	50	155.4	0.43	3.1	48	55	A+Tr HS
D15	0	0	0	88.8	0.43	3.1	23	–	HS+P
D16	0	2	0	88.8	0.43	3.1	23	–	HS+P
D17	0	2	50	88.8	0.65	3.1	3	54	A+HS
D18	0	2	50	88.8	0.75	3.1	3	23	A+HS
D19	60	0	0	88.8	0.43	3.1	–	–	P
D20	300	0	0	88.8	0.43	3.1	–	–	P
D21	600	0	0	88.8	0.43	3.1	–	–	P
D22	0	12	50	88.8	0.43	3.1	3	65	A+Tr HS
D23	3600	0	0	88.8	0.43	3.1	48	20	A+Tr HS

A: NaA; HS: HS; P: NaP; X: NaX, Tr: traces.
[a] (w%) = Na_2CO_3 percentage present in the mixture used for the heat treatment.
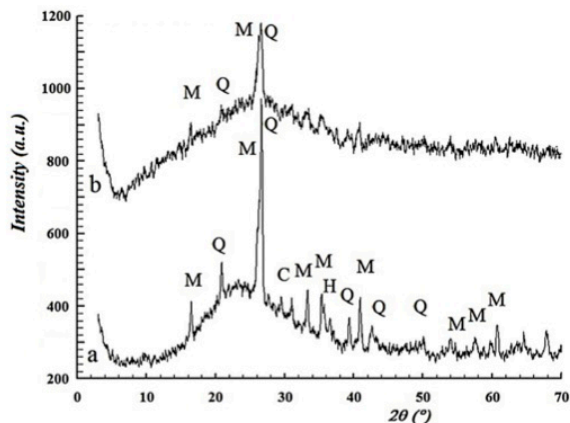[b] weight provided by the extra Al_2O_3 source.

Fig. 1. Fly ash subjected to nonfusion pretreatments. (a) The original fly ash. (b) The solid obtained by milling for 3600 s. Q = quartz, M = mullite, C = calcite, H = hematite.

shows the reduction in height of the main diffraction peaks corresponding to the mineral phases originally present in the fly ash, such as hematite (pdf No. 73-0603), quartz (pdf No. 46-1045) and mullite (pdf No. 79-1457), i.e., a loss of crystallinity occurred, associated with size reduction and particle shape modification [20]. The expansion of the diffraction peaks of quartz and mullite was also detected. This phenomenon was recently related to the formation of nanocrystalline particles by milling [21]. In this case, the appearance of new crystalline phases was not observed. Considering the results obtained in previous work [22,23], longer milling times could enhance ash reactivity towards zeolite formation, despite increased sample contamination due to Fe coming from the attrition of the mill cylinders. In this study, milling times longer than 3600 s were not employed.

On the other hand, important changes in the ash structure were produced by the calcination of ash/sodium carbonate mixtures (50 wt%) as is shown in Fig. 2.

The X-ray maxima corresponding to mullite and quartz, originally present in the fly ash (Fig. 2(a)), completely disappeared
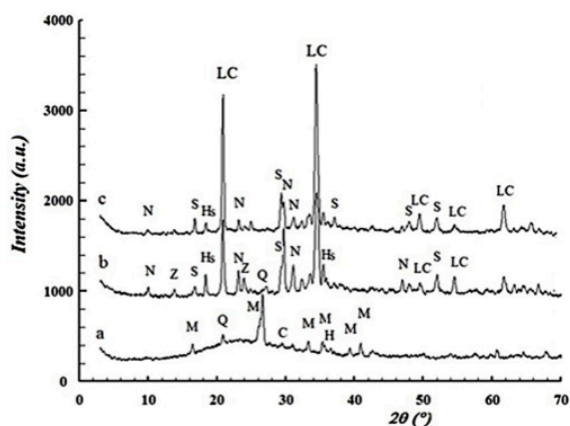
after the alkaline fusion step (Fig. 2(b)). Using the spectrum (a) as reference, after the 2 h alkaline fusion treatment, new phases identified as crystalline aluminosilicates along with a substantial amorphous fraction appeared. The main crystalline phases detected were $NaAlSiO_4$ polymorphs identified by the pdf numbers 19-1176, ascribed to nepheline ($2\Theta = 17.7$, 20.4, 20.6, 21.1, 23.2, 23.5, 27.3, 29.3, 29.7, 31.0, 33.8, 34.9, 36.0, 36.9, . . .), and 11-0221 ascribed to low-carnegieite ($2\Theta = 21.0$, 24.3, 34.6, 40.8, 42.7, . . .). The presence of these crystalline structures was already noticed in our previous work where the fusion pretreatment was applied to activate a residual cracking catalyst [24].

These results are quite different from those obtained using $NaOH$ instead of Na_2CO_3, in a rather more complex fusion treatment previously proposed [25], where an amorphous precursor was formed by the complete collapse of mullite and quartz structures.

The influence of changes in the ash/carbonate ratio used in the heat treatment (800 °C, 2 h) was also analyzed. The heating of ash/sodium carbonate mixtures (75/25 wt%) induced nepheline and low-carnegieite crystallization, and a fraction of the quartz and mullite present in the original fly ash was still remaining. The increase in the ash/sodium carbonate ratio (25/75 wt%) produced a solid whose crystalline composition was identical to that obtained using 50 wt%. Considering these results, the selected carbonate/ash ratio for conducting the synthesis tests was 1.

It is important to note that the solid reorganization also depends on the heating time; the peak intensities corresponding to the new crystalline polymorphs were higher when the heating time was increased to 12 h. The diffraction patterns corresponding to The ash heat-treated by alkaline fusion (50 wt% ash/sodium carbonate ratio) for 2 h and for 12 h are shown in Fig. 2, patterns (b) and (c), respectively. After alkaline fusion at 800 °C, the growth of the new ordered solids was remarkably promoted by an increased heating time. In that way, the generation of significant amounts of low-carnegieite and nepheline was obtained. It is worthy to note that at increased heating time (24 h) the% phase composition remained unaltered, i.e., the percentage of low-carnegieite attained the highest value at 12 h of heating time.

3.2. Hydrothermal synthesis

For the fly ash sample calcined using Na_2CO_3 50 wt% (tests D7 to D14, D17 and D18), the reordering of the crystal arrangement generated the main intermediate structure identified as low-carnegieite, which is present at around 58%. For all the
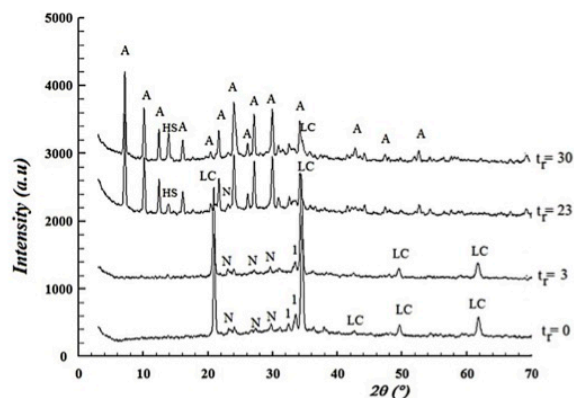

Fig. 2. Influence of fusion pretreatment on the ash crystallinity. XRD patterns corresponding to (a) original fly ash, (b) 50 wt% ash/sodium carbonate mixture calcined at 800 °C for 2 h. (c) 50 wt% ash/sodium carbonate mixture calcined at 800 °C for 12 h. Q = quartz, M = mullite, C = calcite, H = hematite, LC = low-carnegieite, N = nepheline, 1 = $Na_4CaSi_3O_9$, S = sodium silicate/Na_2SiO_3, Hs = Sodium Silicate Hydrate/$Na_2SiO_3 \cdot 9H_2O$; Z = Sodium Aluminum Silicate/$Na_6[AlSiO_4]_6$.

Fig. 3. Evolution of the solid phase in D7 experiment recorded by XRD. t_r = reaction time in hours. LC = low-carnegieite, N = nepheline, 1 = $Na_4CaSi_3O_9$, HS = Hydroxysodalite, A = NaA
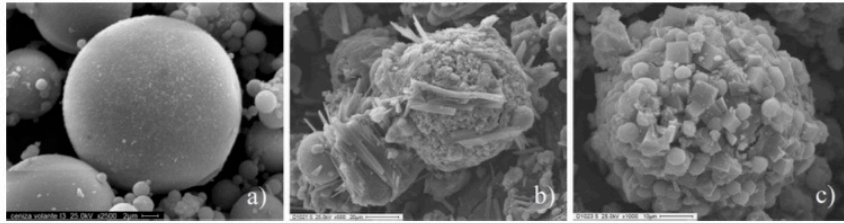
Fig. 4. Morphological evolution of D7 sample: a) original fly ash; b) after aging time, t = 0 h; c) after synthesis, t = 23 h.

hydrothermal synthesis experiments starting from this particular mixture, as the reaction time increased, the peak intensities corresponding to NaA increased, and the peaks corresponding to low-carnegieite decreased.

As an example, Fig. 3 shows the XRD patterns obtained at different reaction times (0, 3, 23, and 30 h) during the hydrothermal synthesis corresponding to the D7 test. After the ageing period at ambient temperature (t_r = 0), a solubilization of some crystalline phases occurred, being the remaining phases identified as low-carnegieite, nepheline and $Na_4CaSi_3O_9$.

After the fusion treatment, the NaA seems to be gradually formed from the soluble silica and alumina species present in the liquid phase and also from the solid polymorphs of $NaAlSiO_2$ previously formed by alkaline fusion.

The crystalline compositions of the different solid phases shown in Fig. 3 were determined by applying the Rietveld analysis. The starting mixture before ageing showed the following compositions: 58.3% of low-carnegieite, 7.1% of nepheline, 7.6% of $Na_4CaSi_3O_9$. At 23 h of reaction the maximum conversion was achieved, resulting in a solid containing 64.0% of NaA, 1.0% of low-carnegieite, 2.2% of nepheline, and 4.6% of Hydroxysodalite. The amorphous fraction detected at t = 0, i.e., after the 48 h of ageing time, is coincident with the fraction obtained at the end of the crystallization. For the whole samples this value oscillated around 22–27%.

Table 1 describes the pretreatments applied and the chemical compositions of the starting mixtures used for the set of synthesis experiments. Considering that the SiO_2/Al_2O_3 ratio detected in the ash is higher than that commonly used for synthesizing NaA, an extra alumina source was added to the synthesis mixture. The effects of changes in the chemical compositions of the starting mixtures on the conversion were analyzed because the effective molar ratios could vary during the crystallization. The solubilization of nutrients originally present in the solid phase, i.e., the silica and alumina fractions emerging from the solid to the liquid phase, could vary with the activation treatment and also with the Na_2O concentration used [26]. Table 1 also shows the values of maximum conversion into NaA, the time needed for reaching these conversions, and also the occurrence of zeolite X (NaX) and/or Hydroxysodalite (HS) cocrystallization. To determine the influence of changes in the initial chemical composition (changes in sodium aluminate, sodium hydroxide, water concentrations) on the percentage of NaA obtained, the starting mixture used in D7 was considered as reference.

By analyzing composition variations with respect to D7, a 25% increase in sodium aluminate concentration (D10 test) allowed reaching the highest conversion at relatively shorter time (64% at 5 h). A similar conversion to that obtained in D7 was reached at a shorter time, when HS also began to appear. This result is similar to that obtained in D22 (65% at 3 h), in which alkaline fusion was

extended for 12 h and the synthesis composition was identical to that used in D7.

Higher alumina concentrations (D17 and D18 syntheses, 50% and 75%, respectively) led to rapid cocrystallization of HS, decreasing NaA growth. For D17, at only 3 h of reaction the main peak at 2θ = 14 corresponding to HS appeared, and a smaller NaA percentage (54%) was obtained compared to D10. In D18, NaA conversion attained a small value at t = 3 h (23%), where the cocrystallization and a further fast growth of HS were observed.

On the other hand, the decrease in alumina concentration (25%, D9) delayed NaA generation, giving the lowest conversion percentage (20%) even at higher reaction times. In addition, NaX began to appear at 31 h of reaction.

Changes of the sodium hydroxide percentage in the activation solution showed the same effects on zeolite conversion as those produced by sodium aluminate variations. It is known that during the aging step and synthesis, the alkalinity of the batch solution plays a significant role by contributing to the dissolution of Si^{4+} and Al^{3+} present in the fly ash [27]. For a 50% increase in alkali concentration (D11), the maximum conversion in/into NaA was reached at shorter times (57% at 3 h) and the appearance of HS was also observed earlier. On the contrary, the 50% decrease in sodium hydroxide concentration (D8) retarded the formation of NaA (57% at 48 h) and improved HS growth.

A decrease in water content (50%, D13) allowed reaching 56% conversion in NaA at shorter reaction time (3 h). Nevertheless, NaA started disappearing as the reaction advanced, giving place to HS formation. On the contrary, as the water content was increased (50%, D12 and 75%, D14), NaA crystallization was progressively delayed (56% at 23 h and 55% at 48 h, respectively).

Samples without any pretreatment prior to the hydrothermal synthesis (D15) led to the formation of HS and NaP-1. In reaction D16 (calcination without Na_2CO_3) at 5 h of reaction, small conversion in NaA was obtained and traces of NaP were also formed. After 30 h of reaction, only HS + NaP were observed; quartz, mullite and albite were additionally detected. It has been further reported that the fusion method favors the production of NaX, or NaA (for an Al rich fly ash), compared to the nonfusion method yielding a mixture of NaP1, NaX and HS [28]. Samples subjected to milling treatment for 60, 300 or 600 s (D19, D20 and D21, respectively) led to zeolite P regardless of the different chemical compositions employed for preparing the starting mixture. For the longest milling time used (D23), a small conversion into NaA (20%) was obtained. It seems that milling times longer than 3600 s were required to produce the ash structural changes needed for improving the silica and alumina reactivity, thus allowing high levels of conversion into NaA. The lack of crystalline ordering as well as the generation of smaller particles produce the broadening and reduction in height of the diffraction peaks, as was observed in the sample obtained at 3600 s milling time.

Table 2
D7 test composition according to the synthesis progress[a].

Oxides, wt%	Na$_2$O	MgO	Al$_2$O$_3$	SiO$_2$	K$_2$O	CaO	TiO$_2$	Fe$_2$O$_3$	SiO$_2$/Al$_2$O$_3$
Fly ash	0.8	1.6	27.4	62.8	0.7	1.8	1.4	3.5	3.87
D7, 0 h	16.6	1.2	28.5	48.6	–	2.0	1.0	2.1	2.89
D7, 3 h	17.3	1.2	30.5	46.6	–	2.2	0.5	1.7	2.56
D7, 23 h	19.7	1.2	31.3	43.6	–	2.3	0.5	1.4	2.35

[a] Average of four determinations.

3.3. Morphological analyses

The original fly ash and the synthesis products were analyzed by SEM. Morphological changes in the surface of the ash particles along with the hydrothermal synthesis D7 are shown in Fig. 4. The original material consisted of rounded, smoothed particles around 100 μm in size (Fig. 4a). Properly activated by fusion and after being aged for 48 h at room temperature in alkaline solution (Fig. 4b), the spheres showed a surface covered by needle-shaped crystals, identified as low-carnegieite and nepheline, according to the X-ray analysis. During the synthesis, the growth of cubic crystals on the particle surface was increasingly detected. For t = 23 h, SEM analysis revealed that the starting fly ash morphology was maintained (spherical particles) and the surface was completely covered by cubic crystals 6 μm in size (Fig. 4c). As cubic crystals are the typical morphology of NaA, these results confirm those obtained by X-ray analysis. It is interesting to note that the conservation of the spherical morphology of ash particles along the whole process indicates a reordering of the solid phase. As was detected in previous work [24], the transformation of low-carnegieite present in the solid phase into NaA implies the reordering of the orthorhombic low-carnegieite network to the cubic lattice of NaA, i.e., the conversion of low-carnegieite to NaA takes place by a direct solid–solid transformation.

3.4. EDX analyses

The semiquantitative SiO$_2$/Al$_2$O$_3$ molar ratio of the original fly ash determined by EDX analysis was 3.87 (Table 2). Considering complete availability of silica and alumina, this value indicated that an extra source of alumina should be used for adjusting the batch synthesis composition to the molar ratios appropriate for obtaining NaA.

Table 2 shows the D7 test composition as the synthesis time advances. It was observed that the SiO$_2$/Al$_2$O$_3$ ratio decreased as reaction time increased, as is expected due to NaA crystallization, whose theoretical SiO$_2$/Al$_2$O$_3$ ratio is 2.

4. Conclusions

The crystallization of NaA strongly depends on the pretreatment applied to the original fly ash, since this step determines the appearance of intermediate structures that favor the generation of this type of zeolite. Starting from a fly ash, high levels of conversion in NaA could be attained when the ash, prior to the hydrothermal synthesis, was subjected to milling or alkaline fusion. These pretreatments convert the crystalline insoluble structures originally present in the fly ash into amorphous or ordered aluminosiliceous intermediates that, afterwards, during the hydrothermal process, can easily be reorganized into zeolite structures. The zeolitization level is limited, at first, by the silica and/or alumina content of the fly ash and its reactivity. The methodology used in the present work constitutes an easy and inexpensive way to obtain a (60 wt%) NaA- rich product. Besides, the chemical composition of the starting mixture used for the synthesis significantly influences the type of zeolite obtained. In that way, the percentage of conversion in zeolite and the reaction times for attaining maximum conversion could be optimized through an adequate selection of these variables.

References

[1] M. Ahmaruzzaman, A review on the utilization of fly ash, Prog. Energy Combust. 36 (2010) 327–363.
[2] S.S. Bukhari, J. Behin, H. Kazemian, S. Rohani, Conversion of coal fly ash to zeolite utilizing microwave and ultrasound energies: a review, Fuel 140 (2015) 250–266.
[3] T. Aldahri, J. Behin, H. Kazemian, S. Rohani, Synthesis of zeolite Na-P from coal fly ash by thermo-sonochemical treatment, Fuel 182 (2016) 494–501.
[4] A.M. Cardoso, M.B. Horn, L.S. Ferret, C.M.N. Azevedo, M. Pires, Integrated synthesis of zeolites 4A and Na–P1 using coal fly ash for application in the formulation of detergents and swine wastewater treatment, J. Hazard. Mater. 287 (2015) 69–77.
[5] M. Visa, Synthesis and characterization of new zeolite materials obtained from fly ash for heavy metals removal in advanced wastewater treatment, Powder Technol. 294 (2016) 338–347.
[6] A.K. Kondru, P. Kumar, T.T. Teng, S. Chand, K.L. Wasewar, Synthesis and characterization of Na-Y zeolite from coal fly ash and its effectiveness in removal of dye from aqueous solution by wet peroxide oxidation, Arch. Environ. Sci. 5 (2011) 46–54.
[7] X. Querol, N. Moreno, J.C. Umaña, R. Juan, S. Hernández, C. Fernandez-Pereira, Application of zeolitic material synthesized from fly ash to the decontamination of waste water and flue gas, J. Chem. Technol. Biotechnol. 77 (2002) 292–298.
[8] X. Zhang, D. Tang, G. Jiang, Synthesis of zeolite NaA at room temperature: the effect of synthesis parameters on crystal size and its size distribution, Adv. Powder Technol. 24 (2013) 689–696.
[9] P.M. Slangen, J.C. Hansen, H. Van Bekkum, The effect of ageing on the microwave synthesis of zeolite NaA, Microporous Mater. 9 (1997) 259–265.
[10] N. Musyoka, L. Petrik, E. Hums, H. Baser, W. Schwieger, In situ ultrasonic monitoring of zeolite A crystallization from coal fly ash, Catal. Today 190 (2012) 38–46.
[11] T.V. Ojumu, P.W. Plessis, L.F. Petrik, Synthesis of zeolite A from coal fly ash using ultrasonic treatment – a replacement for fusion step, Ultrason. Sonochem. 31 (2016) 342–349.
[12] T. Wajima, K. Sugawara, Material conversion from various incinerated ashes using alkali fusion method, Soc. Mater. Eng. Resour. Jpn. 17 (1) (2010).
[13] S. Bukhari, J. Behin, H. Kazemian, S. Rohani, A comparative study using direct hydrothermal and indirect fusion methods to produce zeolites from coal fly ash utilizing single-mode microwave energy, J. Mater. Sci. 49 (2014) 8261–8271.
[14] N. Musyoka, L. Petrik, E. Hums, Ultrasonic assisted synthesis of zeolite A from coal fly ash using mine waters (acid mine drainage and circumneutral mine water) as a substitute for ultra pure water, Conference Mine Water – Managing the Challenges IMWA (2011).
[15] M. Wdowin, M. Franus, R. Panek, L. Badura, W. Franus, The conversion technology of fly ash into zeolites, Clean Technol. Environ. Policy 16 (2014) 1217–1223.
[16] D.W. Breck, Zeolite Molecular Sieves, Wiley, New York, 1974.
[17] H.M. Rietveld, A profile refinement method for nuclear and magnetic structures, J. Appl. Crystallogr. 2 (1969) 65–71.
[18] J. Rodríguez-Carvajal, Recent developments of the program FULLPROF, in commission on powder diffraction (IUCr). Newsletter 26 (Año 2001) 12–19.
[19] M. Gonzalez, N. Firpo, E. Basaldella, Materiales zeolíticos para purificación de aguas obtenidos a partir de catalizadores de cracking agotados, XVI Congreso Argentino De Catálisis (2009).
[20] A.G. Patil, A. Mahendran, S. Anandhan, Nanostructured fly ash as reinforcement in a plastomer-based composite: a new strategy in value addition to thermal power station fly ash, Silicon 8 (2016) 159–173.
[21] R. Hamzaoui, O. Bouchenafa, S. Guessasma, N. Leklou, A. Bouaziz, The sequel of modified fly ashes using high energy ball milling on mechanical performance of substituted past cement, Mater. Des. 90 (2016) 29–37.
[22] R.M. Torres Sánchez, E.I. Basaldella, J.F. Marco, The effect of thermal and mechanical treatments on kaolinite: characterization by XPS and IEP measurements, J. Colloid Interface Sci. 215 (1999) 339–344.

[23] E. Basaldella, R.M. Torres Sánchez, S. Perez, D. Caputo, C. Colella, Zeolite synthesis from clays: effect of impact grinding on kaolinite structure and reactivity, Proceedings of the 12th Inter. Zeo. Conf. Mat. Res. Soc. (1999).

[24] M.R. Gonzalez, A.M. Pereyra, P. Bosch, G. Fetter, V.H. Lara, E.I. Basaldella, Structural and morphological evolution of spent FCC catalyst pellets towards NaA zeolite, J. Mater. Sci. 51 (2016) 5061–5072.

[25] T. Wajima, K. Sugawara, Material conversion from various incinerated ashes using alkali fusion method, Int. J. Soc. Mater. Eng. Resour. 17 (2010) 47–52.

[26] N. Murayama, H. Yamamoto, J. Shibata, Mechanism of zeolite synthesis from coal fly ash by alkali hydrothermal reaction, Int. J. Miner. Process. 64 (2002) 1–17.

[27] E.I. Basaldella, J.C. Paladino, M. Solari, G.M. Valle, Exhausted fluid catalytic cracking catalysts as raw materials for zeolite synthesis, Appl. Catal. B: Environ. 66 (2006) 186–191.

[28] N. Shigemoto, H. Hayashi, K. Miyaura, Selective formation of Na-X zeolite from coal fly ash by fusion with sodium hydroxide prior to hydrothermal reaction, J. Mater. Sci. 28 (1993) 4781–4786.